2015

Temperature dependence of cesium carbonate-doped electron transporting layers on organic light-emitting diodes

Richard Fu
U.S Army Research Laboratory, Adelphi, MD

Eric Forsythe
U.S Army Research Laboratory, Adelphi, MD

Jianmin Shi
U.S Army Research Laboratory, Adelphi, MD

Merric Srour
U.S Army Research Laboratory, Adelphi, MD

Steven Blomquist
U.S Army Research Laboratory, Adelphi, MD

See next page for additional authors

Synthetic Metals 209 (2015) 128–134

Contents lists available at ScienceDirect

Synthetic Metals

journal homepage: www.elsevier.com/locate/synmet

Temperature dependence of cesium carbonate-doped electron transporting layers on organic light-emitting diodes

Richard Fu*, Eric Forsythe, Jianmin Shi, Merric Srour, Steven Blomquist, David Morton

U.S Army Research Laboratory, 2800 Powder Mill Road, Adelphi, MD 20783-1138, USA

ARTICLE INFO

Article history:
Received 4 June 2015
Received in revised form 13 July 2015
Accepted 17 July 2015
Available online xxx

Keywords:
Organic materials
OLED devices
Electroluminescence
Electron transport
Electron injection
Cesium carbonate doping

ABSTRACT

The temperature dependence and electronic transport properties of 1, 3, 5-*tri*(1-phenyl-1H-benzo[d] imidazol-2-yl) phenyl (TPBI) and 8-hydroxyquinoline aluminum (Alq) electron transporting layers (ETL) have been investigated as a function of cesium carbonate (Cs_2CO_3) doping for organic light emitting devices. The current-voltage and light emission characteristics were measured as a function of the Cs_2CO_3 doped ETL thickness at both room temperature and cryogenic (10–300 K). The current density (J) for the Alq:Cs_2CO_3 ETL device increased for an ETL thickness between 100 and 300 Å, with no further increase in the ETL beyond 300 Å, indicating an electron injection limited contact. Conversely, the J for the TPBI:Cs_2CO_3 ETL device did not saturate for increasing ETL thicknesses confirming the TPBI:Cs_2CO_3 devices have a near-ohmic cathode contact. The correlation of current density–voltage (*J–V*) and luminance-voltage (*L–V*) for both Alq:Cs_2CO_3 and TPBI:Cs_2CO_3 devices were studied over temperatures from 10 to 300 K. Both increased with increasing temperature; however, Cs_2CO_3-doped TPBI devices were more effective than Cs_2CO_3-doped Alq devices. The observed differences between Alq and TPBI may be attributed to the exposed nitrogen electron pair in the electronic structure.

Published by Elsevier B.V.

1. Introduction

Research in organic light-emitting diode (OLED) displays has been attaining greater momentum during the last decade due to their capacity to form flexible displays [1]. OLEDs have many advantages including easy processing, robustness and inexpensive foundry compared to inorganic counterparts, and they have emerged as the second most important display technology for commercial applications [2]. OLED-based displays are integrated in many of today's portable phones due to the visual quality, low profile, and low power consumption. These same attributes have led to recent announcements of OLED television technology as well as OLED-based displays integrated on plastic substrates enabling a new generation of information technologies [3]. In particular, the low power consumption of OLED-displays has attracted strong interest for many portable commercial and military applications [4]. In fact, the OLED display is rapidly moving from fundamental research into industrial product, creating many new challenges like lower operation voltage and power consumption, and operating under extreme environmental conditions [5,6]. Research to lower the OLED operating voltage has led to the development of enhanced electron injection with the integration of alkali metals and alkali metal complexes (such as cesium carbonate, Cs_2CO_3) as a sub-monolayer deposited between the organic electron transporting layer (ETL) and the metal cathode [7,8]. Similarly, the enhancement of the electron transport properties of the bulk organic ETL has been demonstrated by co-evaporating alkali metals and complexes with the organic ETL material [9–12].

Furthermore, the users need high performance displays that can withstand the different environmental conditions, which are used in a wide range of sights and vision systems that can be deployed in very different locations with extreme environmental conditions, such as the mountains in winter or the desert in summer. How the device responds to different temperature ambience has also attracted the attention of scientists [13]. A few researchers have been investigated the temperature dependence of 8-hydroxyquinolinato aluminum (Alq) ETLs on OLEDs [14,15]. However, the cryogenic temperature effects of 1, 3, 5-*tri*(1-phenyl-1H-benzo[d]imidazol-2-yl) phenyl (TPBI) ETLs on OLEDs has not yet been explored.

In this paper, we discuss the electron injection and electron transport characteristics of simple bi-layer OLEDs with 2 different ETLs: Alq and TPBI. TPBI has demonstrated blue fluorescent emission and electron transport properties for OLED-based displays [16,17], while Alq is a green OLED. The results in this paper demonstrate different electron transport and injection

* Corresponding author. Fax: +1 301 394 0310.
E-mail address: richard.x.fu.civ@mail.mil (R. Fu).

http://dx.doi.org/10.1016/j.synthmet.2015.07.025
0379-6779/Published by Elsevier B.V.

characteristics between ETLs consisting of TPBI and Alq doped with Cs_2CO_3 at a fixed concentration of 7% by weight. We use Cs_2CO_3-doped Alq and TPBI as the ETL materials to decrease the operating voltage and power consumption, and systematically investigate cryogenic temperature dependence of Cs_2CO_3-doped Alq and TPBI on an OLED. The mechanisms of the charge-transfer (CT) complex in Cs_2CO_3-doped TPBI are discussed, which provides insight into designing future materials and device structure with enhanced performance.

2. Experiment

The ETL organic materials used were Alq, and TPBI, as illustrated in the Fig. 1 along with the energy level diagram for the simple bi-layer devices architecture. In Fig. 1, the energy level alignment for TPBI shows a Highest Occupied Molecular Orbital (HOMO) state at 6.2 eV below the vacuum level as compared to HOMO of 5.8 eV for Alq [16–18]. The 2 ETL organic materials have the same lowest occupied molecular orbital (LUMO) state relative to the vacuum level implying the electron injection barrier is similar for the undoped TPBI and Alq ETL materials.

The OLEDs were fabricated starting with a standard indium-tin-oxide (ITO) coated glass substrate preparations. Six device cells, with 4 identical devices per cell, were fabricated in a single deposition run for the 2 ETL experiments, TPBI and Alq, respectively. A common (750 Å) 4,4′-bis[N-(1-nathyl)-*N*-phenyl-amino]biphenyl (NPB) hole transporting layer was first deposited on the ITO substrates at 2.0×10^{-6} Torr followed by the EML and ETL layers at a total constant thickness of 600 Å, and a common magnesium (Mg)-silver (Ag) (10 parts Mg to 1 part Ag) cathode. For both sets of devices, the EML was the undoped ETL organic material, TPBI and Alq respectively. The 6 device cells for the TPBI and Alq experimental sets were fabricated as follows:

A. ITO/NPB (750 Å)/EML (600 Å)/ETL (0 Å)/Mg:Ag;
B. ITO/NPB (750 Å)/EML (500 Å)/ETL (100 Å)/Mg:Ag;
C. ITO/NPB (750 Å)/EML (300 Å)/ETL (300 Å)/Mg:Ag;
D. ITO/NPB (750 Å) /EML (100 Å)/ETL (500 Å)/Mg:Ag;
E. ITO/NPB (750 Å)/EML (50 Å)/ETL (550 Å)/Mg:Ag;
F. ITO/NPB (750 Å) /EML (0 Å)/ETL (600 Å)/Mg:Ag.

The doped ETL for the 2 experiments was the co-deposition of TPBI or Alq and Cs_2CO_3 at 7% relative molecular weights. The device cells were sealed and the current density as a function of current density-voltage (*J*–*V*) measurements were conducted with a Keithley 2400 source meter and the light emission properties were measured with a Photoresearch 650 spectrophotometer with the Keithley.

Fig. 2 shows the cryogenic temperature test set-up. The OLED is mounted on a copper (Cu) plate in a cryogenic chamber which acts as a sample holder and is capable of being cooled down to 10 K by a helium pump. The silicon (Si) photodetector is mounted inside the chamber about 2–3 mm from the device surface (not in contact with the sample mounting plate) with feedthroughs that connect it to electronics outside of the chamber. The cryogenic chamber was kept at the vacuum of 10^{-6} Torr during the experiment.

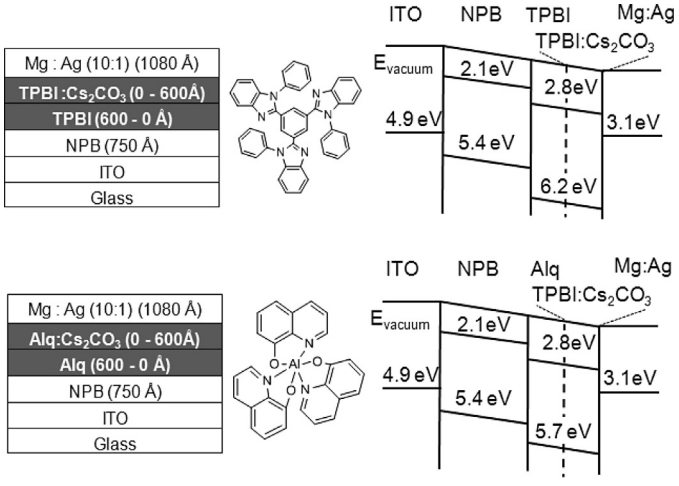

Fig. 1. The TPBI and Alq device configuration with gray regions indicating the thickness ratio of a doped ETL and an undoped emitting layer (EML), where the total ETL+EML layer thickness is constant at 600 Å for all devices investigated. The corresponding energy level diagrams (not including the interface energy level bending) are shown with the TPBI and Alq molecular structures.

3. Results and discussion

3.1. Room temperature characteristics of Cs_2CO_3-doped Alq and TPBI

Fig. 3 shows the current density (*J*) as a function of operating voltage (*V*) (*J*–*V*). Fig. 3a, the Alq:Cs_2CO_3 ETL OLEDs, shows an initial rapid increase in *J* at ETL 100 Å, then slowly increasing until the Alq:Cs_2CO_3 ETL layer is 600 Å (EML = 0 Å). This data point suggests the hole injection into the Alq:Cs_2CO_3 ETL is reduced. By comparison, the TPBI:Cs_2CO_3 *J* continuously increases to the ETL thickness of 600 Å in Fig. 3b.

Fig. 4 is a summary plot of the current density (*J*) at 4 V for the 6 device cells as a function of Alq:Cs_2CO_3 and TPBI:Cs_2CO_3 ETL thickness. *J* at 4 V level off after the Alq ETL doped layer thickness 300 Å. From the inset in Fig. 4, the total contact resistance is represented by R_1, R_{ETL} and represents the resistance of the Alq:Cs_2CO_3 ETL, and R_{EML} is the undoped emission layer Alq EML. As the Alq ETL thickness increases, total resistance, $R_{EML} + R_{ETL}$, will decrease. Thus, the saturation in the current density beyond 300 Å for the Alq:Cs_2CO_3 ETL thickness indicates the contact resistance R_1 dominates the bi-layer electron transport properties as the contact cannot supply additional current as the bulk resistance decreases [18]. Thus, the Alq:Cs_2CO_3 devices are contact limited. Conversely, the TPBI:Cs_2CO_3 devices demonstrate a constant increase in *J* at 4 V as the TPBI:Cs_2CO_3 thickness increases relative to the undoped emission layer TPBI EML. Again, the electron resistance, R_{EML}+R_{ETL} is decreasing and the total device current density, *J*, is increasing, indicating the devices with TPBI:Cs_2CO_3 ETLs are bulk limited, or the contact is near ohmic for all devices. The molecular structures of the TPBI and Alq molecules illustrated in Fig. 1 suggest an explanation for the electron transport differences. The TPBI molecule has 6 N atoms as compared to 3 N atoms in Alq. The addition exposed N electron pairs in TPBI may contribute to improve bulk electron transport properties in Cs_2CO_3-doped devices.

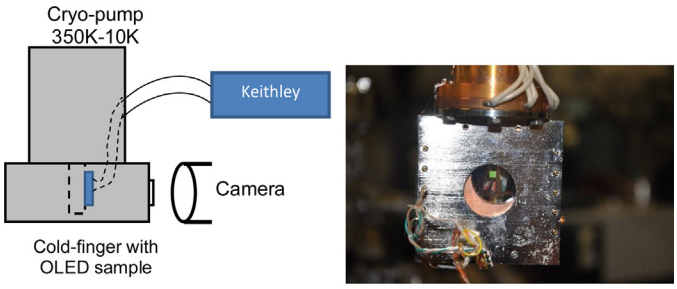

Fig. 2. (a) Schematic of the cryogenic temperature test setup and (b) a close-up of the OLED sample on the cold-finger.

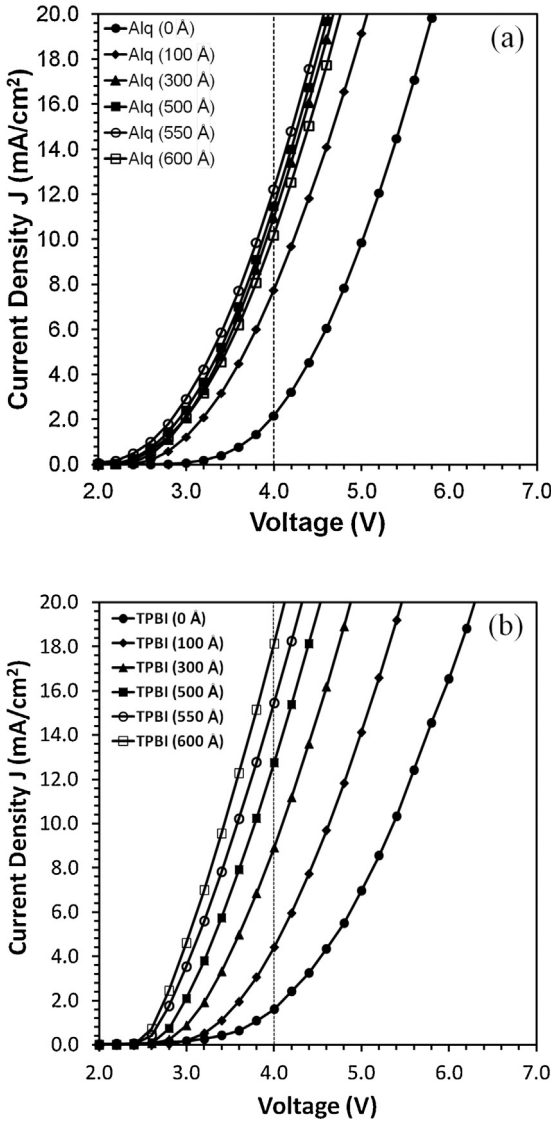

Fig. 3. (a) The *J–V* as increasing thickness of Alq:Cs_2CO_3 ETL, where the EML + ETL = 600 Å. (b) The *J–V* as a function of TPBI:Cs_2CO_3 ETL thickness, where EML + ETL = 600 Å.

The bi-layer device's light-emission properties were measured to further understand how the electron transport properties of Cs_2CO_3-doped ETLs impact the EML. The comparative plot in Fig. 5 indicates the Alq luminance is approximately constant up to an Alq:Cs_2CO_3 ETL thickness of 300 Å and then steadily decreases as the ETL thickness increases (EML decreases). Conversely, the luminance for the TBPI:Cs_2CO_3 devices continues to increase and then abruptly decreases above the ETL thickness of 550 Å. The luminance data confirm the Alq:Cs_2CO_3 device is electron limited between an ETL thickness of 100 to 300 Å. The reported photoemission results confirm the sharp shift in the molecular orbital states at the cathode interface [19]. The steady decrease in Alq:Cs_2CO_3 luminance as the EML thickness decreases from 300 to 500 Å implies a combination of the exciton diffusion length and internal electric field in the undoped Alq EML impacts the luminance. Conversely, the TPBI devices an increased light emission for an EML as thin as 100 Å, indicating the exciton diffusion length to the quenching ETL is less than Alq. Further, the electric-field exciton dissociation effects are less in the TPBI molecules as compared to Alq.

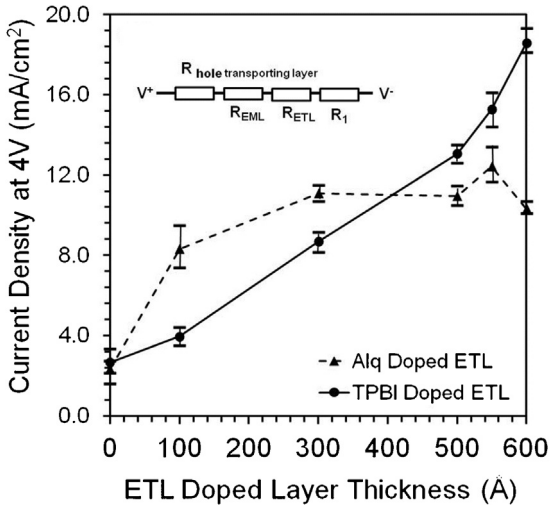

Fig. 4. The average current density, *J*, at 4 V as a function of the Cs_2CO_3-doped ETL for the set of TPBI and Alq devices, where the total ETL + undoped EML thickness is 600 Å, respectively. The error bars indicate the maximum and minimum current density values for the devices at each ETL thickness.

3.2. Temperature dependent J–V characteristics of Cs_2CO_3-doped Alq and TPBI

Figs. 6 and 7 show the temperature-dependent *J–V* characteristics of the devices from the temperature 10 to 300 K for Cs_2CO_3 doped Alq and TPBI, respectively. The current densities are dramatically increased with increasing the temperature due to the increase in mobility and decrease in materials resistivity with increasing temperature at different ETL thicknesses.

The *J–V* curves fit well with the trap charge limited (TCL) current model proposed by Shen et al. [20,21]. Based on the model, the TCL current density is in power law with the applied voltage, and can be expressed as:

$J_{TCL} \sim \frac{V^{m+1}}{d^{2m+1}}$ where power law coefficient $m = T_t/T, T_t = E_t/k$, E_t is the characteristic trap energy, k is the Boltzmann constant, T_t is the characteristic temperature of the exponential trap distribution, and d is the EML thickness which is 600 Å minus the ETL thickness.

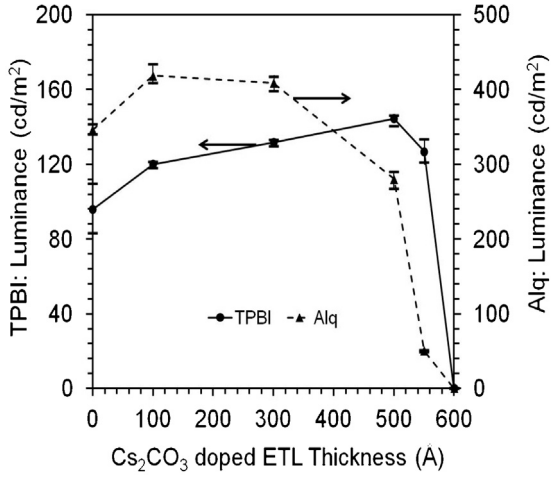

Fig. 5. The total average luminance at 20 mA/cm^2 for TPBI (CIE: 0.15, 0.10) and Alq (CIE: 0.33, 0.54) based devices as a function of Cs_2CO_3-doped ETL thickness, where the total EML+ETL thickness is 600 Å. The error bars indicate the maximum and minimum luminance values for the device sets at each ETL thickness.

With the codeposited Alq/TPBI + 7% Cs_2CO_3 ETL, the current density is constantly increased with increasing the codeposited ETL thickness since $d = 600$ Å – ETL thickness is decreasing. Cs_2CO_3 has been shown a very efficient electron injection material in OLEDs, including in OLEDs based on Alq/TPBI. Compared to undoped TPBI devices, it has been shown that devices using a Cs_2CO_3 electron injection layer have a lower operating voltage and power consumption across the temperature range from 10 to 300 K at 20 mA/cm^2, as specified in Figs. 6 and 7. The operating voltage is decreased with increasing doped ETL from 0 to 500 Å.

3.3. Temperature dependent electroluminescence (EL) of Cs_2CO_3-doped Alq and TPBI

The luminance-voltage (L–V) characteristics are shown in Figs. 8 and 9. The luminance increases with temperature at different ETLs. The electron mobility increases with increasing temperature. The mobility of electrons is critically important to recombination at the NPB/Alq or TPBI interface. The speculation is that the holes and electrons need to combine to form excitons at the NPB/Alq or TPBI interface, and this process is driven by the

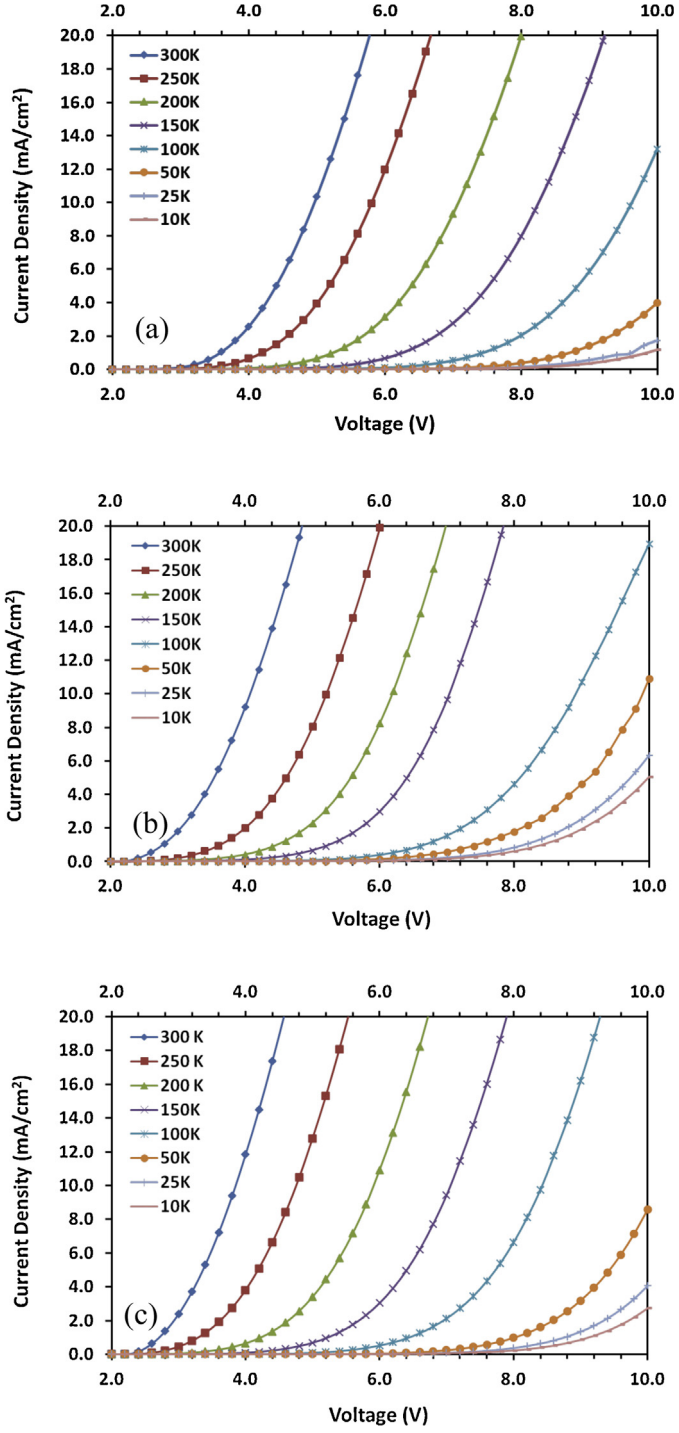

Fig. 6. J–V curves of Cs_2CO_3-doped Alq at different temperatures (10–300 K): (a) ETL = 0 Å, (b) ETL = 300 Å, and (c) ETL = 500 Å.

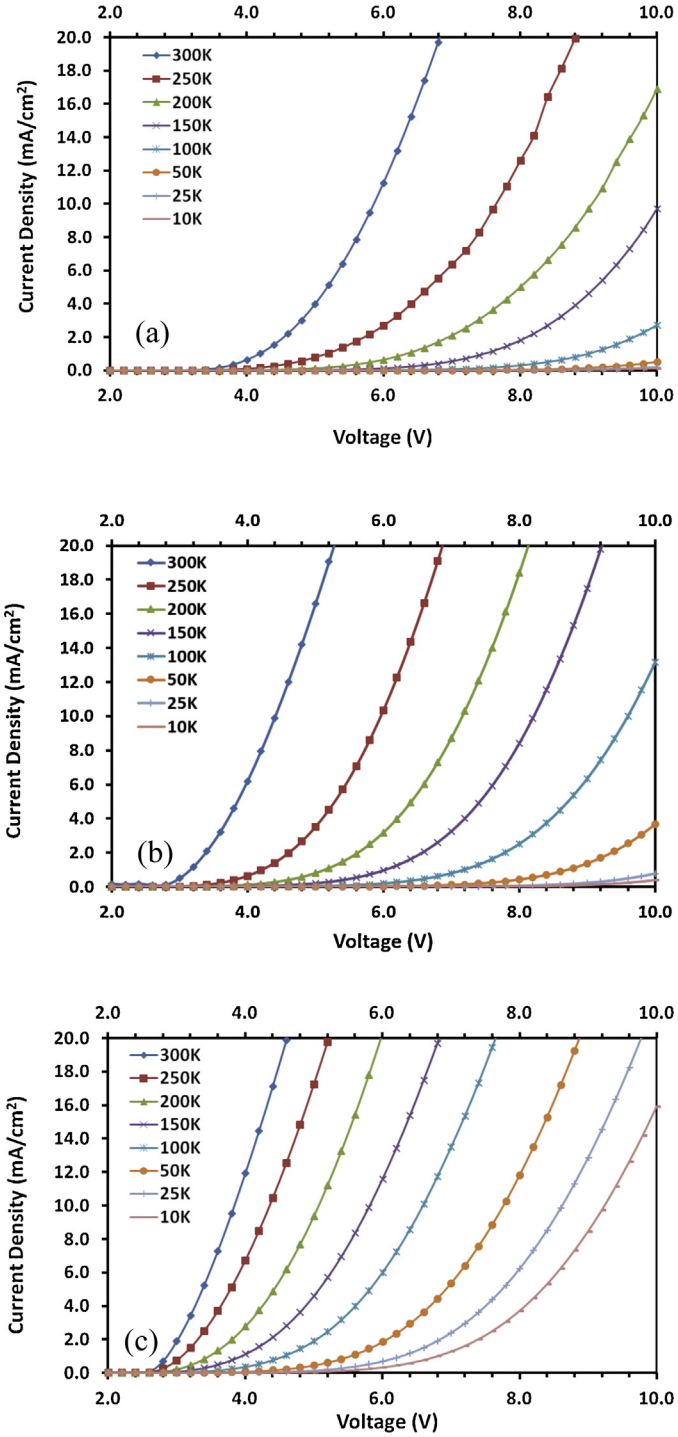

Fig. 7. J–V curves of Cs_2CO_3-doped TPBI at different temperatures (10–300 K): (a) ETL = 0 Å, (b) ETL = 300 Å, and (c) ETL = 500 Å.

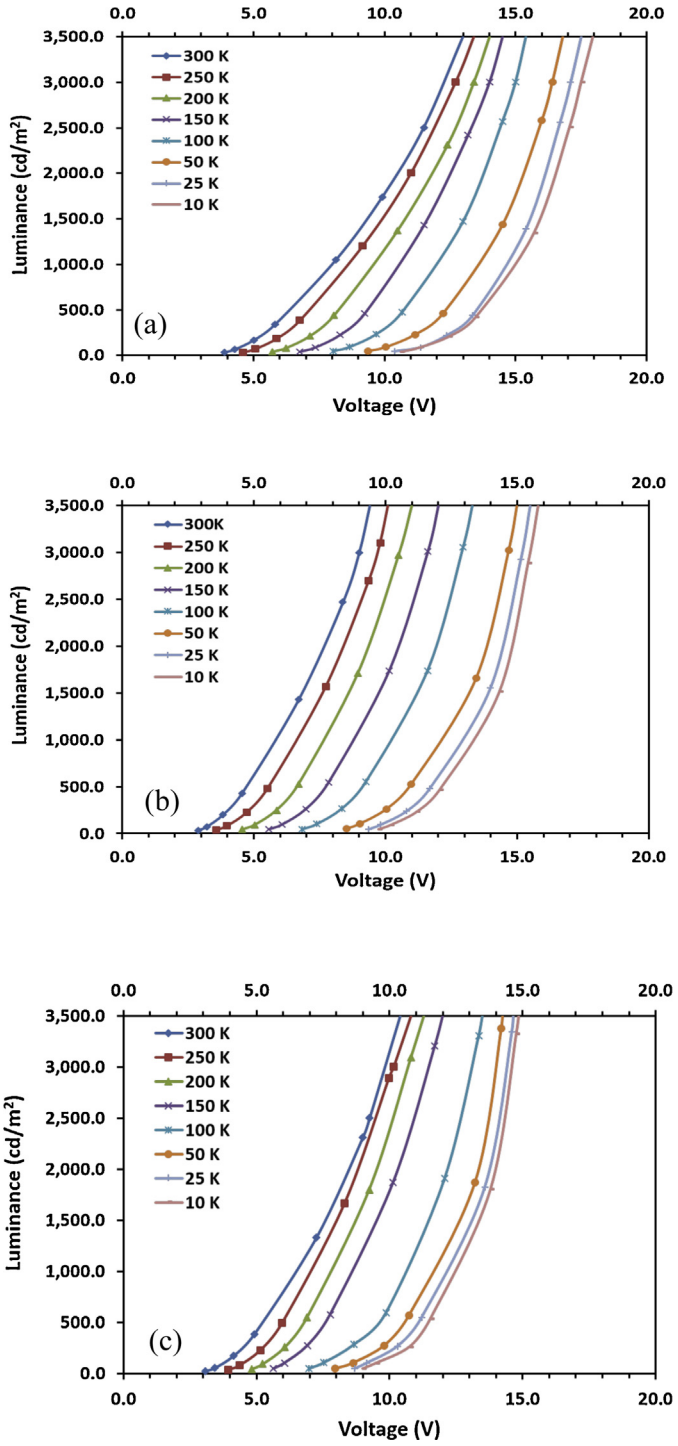

Fig. 8. *L–V* curves of Cs_2CO_3-doped TPBI at different temperatures (10–300 K): (a) ETL = 0 Å, (b) ETL = 300 Å, and (c) ETL = 500 Å.

transportation of the slower electrons from Alq or TPBI. The increasing flux of electrons to the interface with temperature is driven by the increasing mobility of the electrons with temperature. Therefore, the temperature dependence of the electroluminescence (EL) performance resulted from the temperature dependence of the electron mobility.

The luminance also increased with increasing Cs_2CO_3-doped ETL from 0 to 500 Å. As indicated in Fig. 3 and 4, current density, *J*, increased with increasing Cs_2CO_3-doped ETL and flatted out at ETL 300 Å for Alq:Cs_2CO_3, which was matched by *L–V* plots in Fig. 10. Conversely, *J* kept increasing with increasing ETL for TPBI:Cs_2CO_3, which suggested that the device with Cs_2CO_3-doped ETL are bulk limited. The operating voltage for the Cs_2CO_3-doped TPBI measured a continuous decrease as the ETL thickness increased relative the EML [22], indicating a near ohmic contact. Importantly, the Cs_2CO_3-doped ETL luminance output continued to increase to an ETL thickness beyond 500 Å. These results demonstrate an OLED can be optimized with a thick TPBI ETL and a lower operating voltage.

It was well recognized that the electron mobility in the ETL (Alq or TPBI) is less than the hole mobility in hole transport layer (NPB),

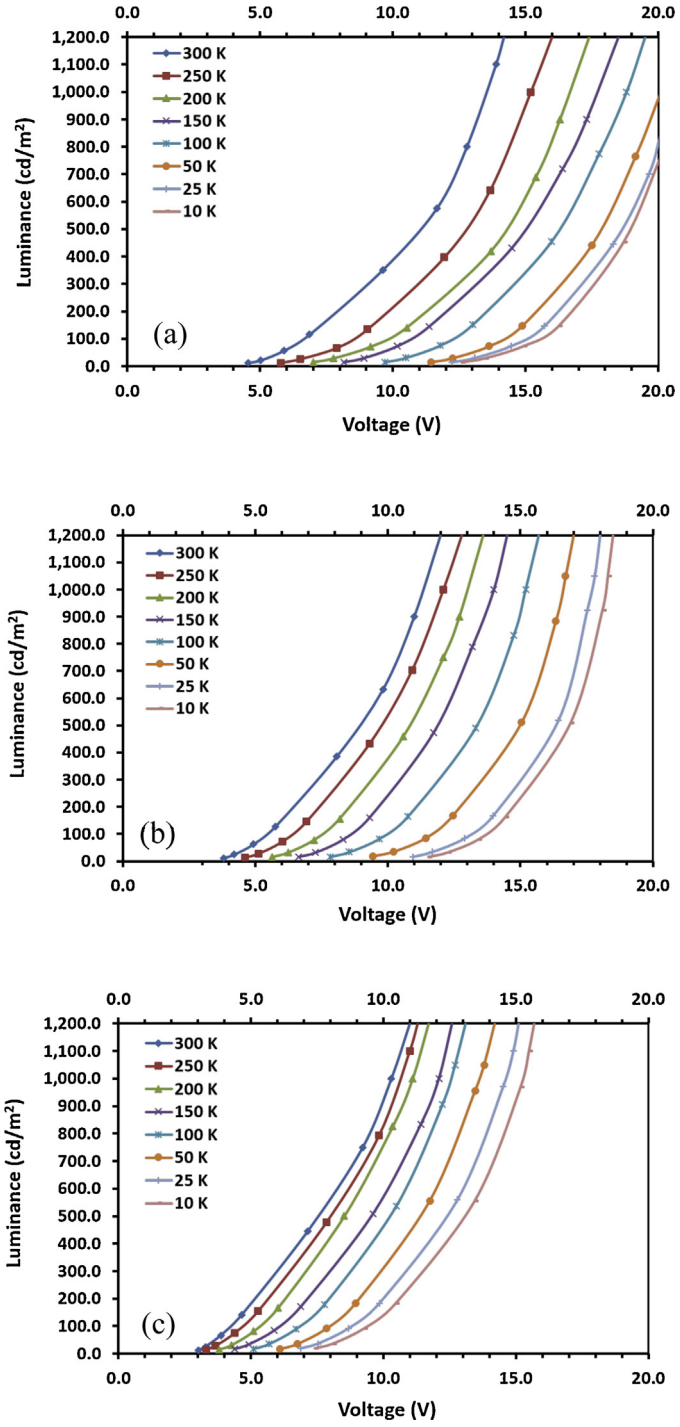

Fig. 9. *L–V* curves of Cs_2CO_3-doped TPBI at different temperatures (10–300 K): (a) ETL = 0 Å, (b) ETL = 300 Å, and (c) ETL = 500 Å.

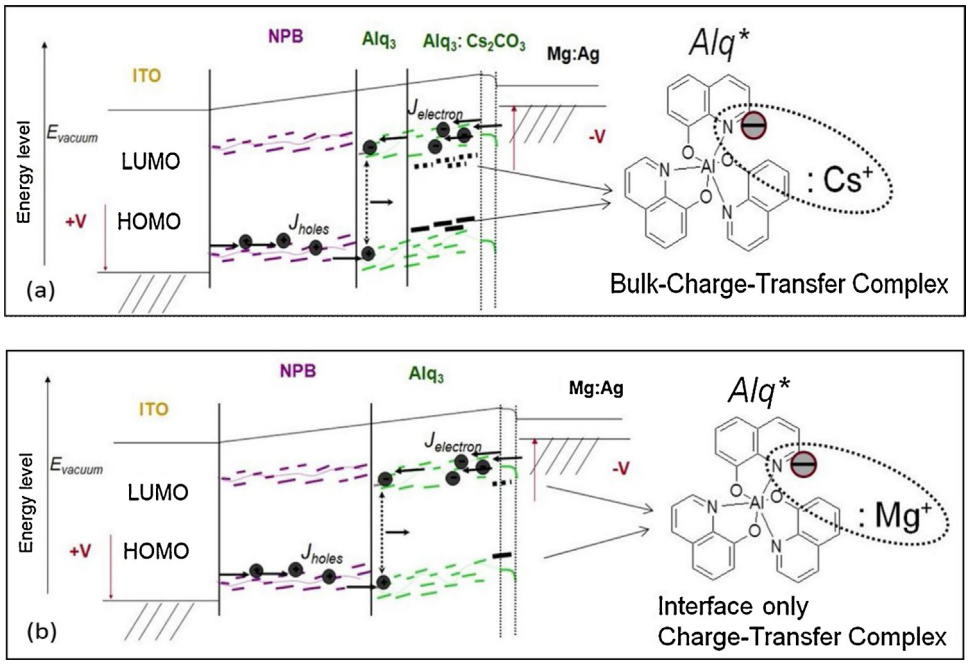

Fig. 10. Cs_2CO_3-doped Alq CT complex: (a) bulk-CT complex with ETL; (b) interface only CT complex without ETL.

and those difference was also observed in the different temperature ranges [23,24]. Therefore, the EL performance is controlled by the slower electrons. In this work, we doped the ETL, Alq or TPBI, with Cs_2CO_3 to increase electrons and their mobility, and balance electrons and holes by tuning the Cs_2CO_3-doped Alq or TPBI ETL thickness [22]. Several photoemission studies have reported the role of Cs_2CO_3-doped Alq ETL OLED. In particular, Li et al. employed a quartz-crystal microbalance to monitor the decomposition of Cs_2CO_3 in situ and elucidated that Cs_2CO_3 decomposes to metallic Cs during thermal evaporation, and that the low work function metal Cs is responsible for the enhanced electron injection. The metallic cesium mechanism reveals that Cs_2CO_3 has a superior electron injection ability regardless of the cathode metal [25]. Duan et al. indicated that Cs_2CO_3 with low evaporation temperatures would decompose and release low work function metal Cs during evaporation, enabling promising electron injection for OLEDs [26]. The enhanced electron injection is associated with a strong n-doping effects and increase of electron concentrations in the ETL induced by Cs_2CO_3. Since such a reaction occurs without the presence of metals, cathode structures incorporating Cs_2CO_3 may be applied to a wide range of electrode materials. However, different ETLs (Alq or TPBI) did affect the properties of OLED devices. Chan et al. reported that the performance of the n-type layers depends on their electrical conductivities which can be improved by using an electron-transporting host with higher electron mobility [27]. Therefore, the higher mobility of TPBI OLED could be one of the reasons for its superior performance.

The photoemission studies have demonstrated that the alkali metal cesium (Cs) contributes to a charge transfer (CT) in interaction with the N 1 s atoms in Alq organic molecules [28,29]. Fig. 10 demonstrated the mechanisms of Cs_2CO_3-doped Alq ETL. Fig. 10a showed the Cs_2CO_3 transfers an electron to nitrogen in the Alq, which cause the molecules twisted and distorted. Due to this distortion the molecule has higher energy and is called Alq* with an extra electron. This process is defined as bulk-CT complex, which is happened with Cs_2CO_3 doping. Those Alq* have free electrons to improve electron mobility and decrease the resistance. Furthermore, Alq has fewer nitrogen electron pairs (3 N) exposed contributing to enhanced bulk-CT complex and electron mobility compared to TPBI (6 N) in Fig. 1. However, the interface-CT complex is happened on the interface between undoped Alq and cathode Mg/Ag in Fig. 10b. These results show that nitrogen-group organic molecule conjugation is critical for the design for improved electron transport, and the addition of exposed N electron pairs in TPBI may contribute to improve bulk electron transport properties in Cs_2CO_3-doped devices, which also explained that Cs_2CO_3-doped TPBI were more effective than Cs_2CO_3-doped Alq devices from Figs. 3-9.

Hu et al. studied the temperature-dependent EL and electron mobility of the OLED with the structure ITO/poly(3,4-ethylenedioxythiophene) (PEDOT) (50 nm)/*N,N′*-diphenyl-*N,N′*-*bis*(3-methylphenyl)-1,1′-biphenyl-4,4′-diamine (TPD) (50 nm)/Alq (60 nm)/lithium fluoride (LiF) (1 nm)/aluminum (Al) (90 nm) [30]. They indicated that although the electron mobility almost triples with the temperature increasing from 60 to 220 K, it still cannot catch up with the holes accumulations at the interface. As the hole density increases with temperature, the charge balance factor deteriorates due to the accumulation of the holes at the TPD/Alq interface. EL efficiency saturated below 220K and decreases above that, and electron mobility, EL intensity had a maximum around 220 K. However, in our study, the temperature dependence of EL for Cs_2CO_3-doped Alq or TPBI showed that the charge balance factor monotonically increases with increasing temperature. The EL performance expressed the consistent temperature dependence over the whole temperature range (10–300 K), resulting from increasing electrons and their mobility. The temperature dependence of the electron mobility may attribute to an optimal physical alignment among organic molecules that encourages charge transport.

4. Conclusion

We have demonstrated different thickness dependence on the operating voltage and temperature dependence on the current density and luminance for Alq:Cs_2CO_3 ETLs as compared to TPBI:Cs_2CO_3 ETLs. The current density for the Alq:Cs_2CO_3 ETL OLED increased for ETL thickness from 100 to 300 Å. Beyond the ETL thickness of 300 Å, the current density did not show further

increase. The results indicate Alq:Cs_2CO_3 ETL thickness greater than 300 Å are electron injection limited. The current density for the TPBI:Cs_2CO_3 measured a continuous increase as the ETL thickness increased, indicating a near ohmic contact. Importantly, the TPBI:Cs_2CO_3 luminance output continued to increase to an ETL thickness beyond 500 Å. These results demonstrate an OLED can be optimized with a thick TPBI ETL and a lower operating voltage as compared to an Alq OLED with a Cs_2CO_3-doped ETL.

The temperature-dependent *J–V* and *L–V* characteristics for both Alq:Cs_2CO_3 and TPBI:Cs_2CO_3 devices were investigated. The temperature-dependent *J–V* characteristics demonstrated that current density increased with increasing temperature from 10 to 300 K and increasing Cs_2CO_3-doped ETL thickness, which fit well with the TCL current model. The EL performance increased with increasing temperature monotonically over the whole temperature range (10–300 K). The temperature dependence of the electron mobility may attribute to an optimal physical alignment among Alq or TPBI molecules that encourages charge transport. The observed difference between the Alq:Cs_2CO_3 ETL and TPBI:Cs_2CO_3 ETL devices may be attributed to the number of exposed nitrogen electron pairs in the electronic structure that can contribute to the CT complex with the Cs atoms.

References

[1] J.H. Burroughes, et al., Light-emitting diodes based on conjugated polymers, Nature 347 (1990) 539.
[2] G. Yu, A.J. Heeger, High efficiency photonic devices made with semiconducting polymers, Synth. Met. 85 (1997) 1183.
[3] B. O'Brien, et al., 14. 7 Active Matrix PHOLED Displays on Temporary Bonded PEN Substrates with Low Temperature IGZO TFTs, SID Symp. Digest Tech. Papers 1 (2013) 447.
[4] S.M. O'Rourke, et al., Direct fabrication of A-Si:H thin film transistor arrays on plastic and metal foils for flexible displays, Inf. Disp. 10 (2008) 18.
[5] J.S. Swensen, et al., Blue phosphorescent organic light-emitting devices utilizing cesium–carbonate-doped 2,4,6-tris(2′,4′-difluoro-[1,1′-biphenyl]-4-yl)-1,3,5-triazine, J. Photonics Energy 1 (2011) 011008.
[6] D.A. Fellowes, M.V. Wood, AMOLED (active matrix OLED) functionality and usable lifetime at temperature, Proc. of SPIE, Vol. 5800 (2005) 138.
[7] M.A. Baldo, et al., Highly efficient phosphorescent emission from organic electroluminescent devices, Nature 395 (1998) 151.
[8] L.S. Hung, C.W. Tang, M.G. Mason, Enhanced electron injection in organic electroluminescence devices using an Al/LiF electrode, Appl. Phys. Lett. 70 (1997) 152.
[9] T. Wakimoto, et al., Organic EL cells using alkaline metal compounds as electron injection materials, IEEE Trans. Electron. Dev. 44 (1997) 1245.
[10] G.E. Jabbour, et al., Aluminum based cathode structure for enhanced electron injection in electroluminescent organic devices, Appl. Phys. Lett. 73 (1998) 1185.
[11] J. Kido, T. Matsumoto, Bright organic electroluminescent devices having a metal-doped electron-injecting layer, Appl. Phys. Lett. 73 (1998) 2866.
[12] M. Pfieffer, et al., Doped organic semiconductors: physics and application in light emitting diodes, Org. Electron. 4 (2003) 89.
[13] T.W. Lee, O.O. Park, The effect of different heat treatments on the luminescence efficiency of polymer light-emitting diodes, Adv. Mater. 12 (11) (2000) 801.
[14] H. Aziz, Z.D. Popovic, N.-X. Hu, Organic light emitting devices with enhanced operational stability at elevated temperatures, Appl. Phys. Lett. 81 (2) (2002) 370.
[15] T.A. Shahul Hameed, P. Predeep, M.R. Baiju, in: P. Predeep (Ed.), Organic Light Emitting Diodes: Device Physics and Effects of Ambience on Performance Parameters, Optoelectronics-Devices and Applications, InTech, 2011 ISBN: 978-953-307-576-1.
[16] J. Shi, C.W. Tang, and C.H. Chen, Blue organic electroluminescent devices, U.S. Patent No. 5645,948 (1997).
[17] Z. Gao, C.S. Lee, I. Bello, S.T. Lee, R.-M. Chen, T.-Y. Luh, J. Shi, C.W. Tang, Supramolecular photosensitive and electroactive materials, Appl. Phys. Lett. 74 (1999) 865.
[18] M. Abkowitz, J.S. Facci, J. Rehm, Direct evaluation of contact injection efficiency into small molecule based transport layers: Influence of extrinsic factors, J. Appl. Phys. 83 (1998) 2670.
[19] M.G. Mason, C.W. Tang, L.-S. Hung, P. Raychaudhuri, J. Madathil, L. Yan, Q.E. Le, Y. Gao, S.-T. Lee, L.S. Liao, C.F. Cheng, W.R. Salaneck, D.A. dos Santos, J.L. Bredas, Interfacial chemistry of Alq_3 and LiF with reactive metals, J. Appl. Phys. 89 (2001) 2756.
[20] Z. Shen, P.E. Burrows, V. Bulovic, S.R. Forrest, M.E. Thompson, Three-color, tunable, organic light-emitting devices, Science 276 (1997) 2009.
[21] P.E. Burrows, Z. Shen, V. Bulovic, D.M. McCarty, S.R. Forrest, J.A. Cronin, M.E. Thompson, Relationship between electroluminescence and current transport in organic heterojunction light-emitting devices, J. Appl. Phys. 79 (1996) 7991.
[22] R. Fu, et al., Improvement of device efficiency for blue organic light emitting diodes by controlling the Cs_2CO_3-doped electron transport layer, J. Photonics Energy 4 (2014) 043595.
[23] S.W. Tsang, S.K. So, J.B. Xu, Application of admittance spectroscopy to evaluate carrier mobility in organic charge transport materials, J. Appl. Phys. 99 (2006) 013706.
[24] C.-C. Wu, et al., Hole-transport properties of a furan-containing oligoaryl, J. Appl. Phys. 93 (2003) 5465.
[25] Y. Li, et al., Elucidation of the electron injection mechanism of evaporated cesium carbonate cathode interlayer for organic light-emitting diodes, Appl. Phys. Lett. (2015) 90.
[26] L. Duan, et al., Progress on efficient cathodes for organic light-emitting diodes, J. Soc. Inf. Disp. 19 (2011) 453.
[27] M.Y. Chan, et al., Influences of connecting unit architecture on the performance of tandem organic light-emitting devices, Adv. Funct. Mater. 17 (2007) 2509.
[28] C.I. Wu, et al., Electronic structures and electron-injection mechanisms of cesium carbonate-incorporated cathode structures for organic light-emitting devices, Appl. Phys. Lett. 88 (2006) 152104.
[29] H. Ding, Y. Gao, Electronic structure of Cs-doped *tris*(8-hydroxyquinoline) aluminum, Appl. Phys. Lett. 86 (2005) 213508.
[30] H. Mu, et al., Temperature dependence of electron mobility, electroluminescence and photoluminescence of Alq3 in OLED, J. Phys. D 41 (2008) 235109.